Equilibrium Structures and Vibrational Assignments for Isoamyl Alcohol and *tert*-Amyl Alcohol: A Density Functional Study

Wolfgang Förner and Hassan M. Badawi

Department of Chemistry, King Fahd University of Petroleum and Minerals, Dhahran 31261, Saudi Arabia

Reprint requests to Wolfgang Förner. E-mail: forner@kfupm.edu.sa

Z. Naturforsch. **2013**, *68b*, 841 – 851 / DOI: 10.5560/ZNB.2013-3003
Received February 9, 2013

We have calculated the vibrational spectra of isoamyl alcohol and of *tert*-amyl alcohol using Density Functional Theory (DFT) with the Becke-3 Lee Yang Parr (B3LYP) functional and a 6-311+G** atomic basis set. The energies of the conformers were also calculated with *ab initio* Perturbation Theory of second (MP2) and fourth order restricted to single, double and quadruple excitations (MP4 SDQ) with the same basis set. We found rather complicated equilibria of four conformations in each case, counting only those with appreciable abundancies. PED data were compared with GAUSSVIEW animations. The calculated wavenumbers agree rather well with the experimental ones when the *gauche-trans* conformer is assumed as the most important one for isoamyl alcohol, and the *gauche-gauche* one for *tert*-amyl alcohol. However, some of the experimental bands had to be assigned also to other conformers, indicating their presence in the equilibrium mixture. Due to sterical reasons both the CO and the OH bonds appear to be weaker in the tertiary alcohol, considering the wavenumbers of the CO and OH bond stretching vibrations. The bond lengths point into the same direction, however, the OH bond in the tertiary alcohol is only slightly longer than that in the primary alcohol.

Key words: Isoamyl Alcohol, *tert*-Amyl Alcohol, Vibrational Assignments, Molecular Structures, DFT Study

Introduction

Vibrational assignments of infrared and Raman lines in the respective spectra are a very important tool, both for detection of the presence of chemicals in reaction mixtures and for the study of atomic motions in molecules. The best way to perform such assignments are potential energy distribution (PED) calculations [1] which yield not only the presence of a group coordinate (the symmetry coordinates, when symmetry is present), but also quantitatively its degree of admixture in a normal mode. In this work we study both PED calculations and the results of the more qualitative GAUSSVIEW program [2]. We find that although GAUSSVIEW yields no quantitative information at all, it works rather well as long as the degree of mixing of different group coordinates in a normal mode is not too large, *i. e.* in relatively small molecules. Further we discuss structures and PEDs as obtained from Density Functional Theory (DFT) calculations.

To this end we were looking for molecules which are both relatively small but also of some chemical and/or biological importance. Thus we have chosen isoamyl alcohol (3-methylbutan-1-ol) and *tert*-amyl alcohol (2-methylbutan-2-ol) as our systems. These molecules allow a look at the different behavior of primary and tertiary OH groups. We have also calculated amylalcohol, but because of it being a primary alcohol like isoamyl alcohol we did not expect anything new from this system, which turned out to be the case and thus we restrict our discussion to *tert*- and isoamyl alcohol.

Isoamyl alcohol has some biological significance and because we are not aware of any literature about the vibrational spectroscopy or about any calculations of structural equilibria, we think that this should be mentioned in the Introduction. For example there is even a gene for isoamyl alcohol oxidase in Aspergillus oryzae [3], and it is known that there are differences in metabolism and DNA ethylation between it and ethanol [4]. Further there is decarboxylation of α-

ketoisocaproate to isoamyl alcohol formation [5] and isoamyl alcohol-induced morphological change [6] in Saccharomyces cerevisiae. A sake yeast mutant produces isoamyl alcohol [7]. Finally there is a fragrance materials review on isoamyl alcohol [8]. On the chemical side there is for example a catalytic study of isoamyl alcohol dehydrogenation [9] and a kinetic study of the esterification of acetic acid with isoamyl alcohol [10].

tert-Butylalcohol (being a tertiary alcohol as our system, *tert*-amyl alcohol) is reported to undergo microbial biodegradation [11], the solubility of fuel oxygenates in water is studied as a function of its concentration [12], and in reactive distillation it is used in glycerol ether synthesis [13]. In a thermodynamic study excess enthalpies of binary and ternary mixtures containing *tert*-amyl alcohol were determined [14]. Again in reactive distillation it was etherized with ethanol [15], and further phenol was alkylated with *tert*-amyl alcohol using a superacidic mesoporous catalyst [16]. Tertiary alcohols were used as reaction media in nucleophilic fluorinations [17, 18] and finally a kinetic study of the liquid phase synthesis of *tert*-amyl ethyl ether was performed [19].

Experimental Spectra

The sample of liquid isoamyl alcohol with about 98 % purity was purchased from BDH Chemicals. The mid-infrared spectrum (4000 – 500 cm^{-1}) of the chemical was obtained with a Perkin Elmer 16F PC FTIR spectrometer using an NaCl window. Finally further experimental spectra of the two molecules had to be retrievd from the official Japanese vibrational spectroscopy link http://www.aist.go.jp/RIODB/SDBS, no. 541 in case of the Raman spectrum of isoamyl alcohol and no. 1709 in case of the infrared and Raman spectra of *tert*-amyl alcohol to compare our calculated wavenumbers with the experimental ones.

Theoretical Calculations

For our DFT calculations we used the GAUSSIAN 03 program system and the 6-311+G** atomic basis set [20]. We set up internal and group (symmetry if there would be a symmetry) coordinates which are given in Tables S1 and S2 (S before a figure or table number indicates that it is part of the Supporting Information available online; see note at the end of the paper for availability), while the structures of the molecules as calculated with DFT as well as the atom numbering

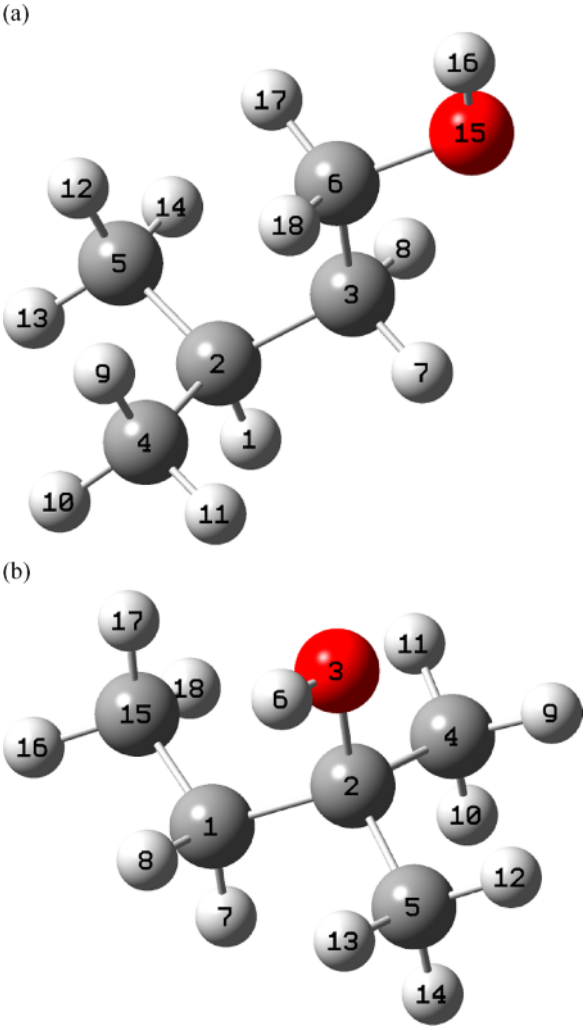

Fig. 1. Atom numbering of the *trans-trans* structure of isoamyl alcohol (upper panel) and the *gauche-gauche* structure of *tert*-amyl alcohol (lower panel).

used are drawn in Fig. 1. With the help of these coordinates and the GAUSSIAN output we were able to calculate the PEDs using our program [1].

Conformational Equilibria and Structural Data

Isoamyl alcohol exists in a conformational equilibrium of four conformers at 25 °C. The relative energies of the conformers for both alcohols are listed in Table 1. Due to the fact that *gauche* conformers are degenerate, the conformer lowest in energy, the

Table 1. Relative energies E_r (kcal mol^{-1}) for the different conformers of isoamyl alcohol (torsion angles T_c = $C_6C_3C_2H_1$, T_o = $O_{15}C_6C_3C_2$ and T_{oh} = $H_{16}O_{15}C_6C_3$) and of *tert*-amyl alcohol (torsion angles T_o = $C_{15}C_1C_2O_3$ and T_{oh} = $H_6O_3C_2C_1$). DFT denotes Density Functional Theory with Becke 3 Lee Yang Parr functional, MP2 Moeller Plesset Perturbation Theory of second order, and MP4 SDQ Moeller Plesset Perturbation Theory of fourth order with single, double and quadruple excitations. Abundancies are based on MP4 SDQ energies.

Isoamyl alcohol				
	T_o (deg)	T_c (deg)	T_{oh} (deg)	E_r (kcal mol^{-1})
	trans-trans (24 % abundance)			
DFT	180.0	180.0	180.0	0.00
MP2	180.0	180.0	180.0	0.10
MP4 SDQ	180.0	180.0	180.0	0.00
	gauche-gauche (32 % abundance)			
DFT	65.7	172.2	61.5	0.42
MP2	61.4	166.8	59.0	0.25
MP4 SDQ	62.0	167.7	59.2	0.25
	gauche-trans (43 % anbundance)			
DFT	170.2	67.4	177.5	0.42
MP2	164.3	61.7	175.7	0.00
MP4 SDQ	165.2	62.3	176.0	0.07
	trans-cis (2 % abundance)			
DFT	180.0	180.0	0.0	1.30
MP2	180.0	180.0	0.0	1.59
MP4 SDQ	180.0	180.0	0.0	1.49
tert-Amyl alcohol				
	T_o (deg)		T_{oh} (deg)	E_r (kcal mol^{-1})
	gauche-gauche (52 % abundance)			
DFT	58.6		64.4	0.00
MP2	61.1		64.1	0.00
MP4 SDQ	60.9		63.8	0.00
	cis-cis (5×10^{-4} % abundance)			
DFT	0.0		0.0	5.76
MP2	0.0		0.0	6.57
MP4 SDQ	0.0		0.0	6.43
	cis-trans (10^{-2} % abundance)			
DFT	0.0		180.0	4.14
MP2	0.0		180.0	4.75
MP4 SDQ	0.0		180.0	4.55
	trans-cis (2 % abundance)			
DFT	180.0		0.0	1.37
MP2	180.0		0.0	1.45
MP4 SDQ	180.0		0.0	1.50
	trans-gauche (33 % abundance)			
DFT	177.2		59.1	0.23
MP2	177.4		57.1	0.22
MP4 SDQ	177.6		57.5	0.26
	trans-trans (13 % abundance)			
DFT	180.0		180.0	0.29
MP2	180.0		180.0	0.22
MP4 SDQ	180.0		180.0	0.39

Table 2. Observed and calculated wavenumbers in isoamyl alcohol (most observed wavenumbers fit well with the calculated ones of the *gauche-trans* conformation) and *tert*-amyl alcohol (most observed wavenumbers fit nicely with the calculated ones of the *gauche-gauche* conformation). However, both alcohols seem to exist in a mixture of several low-energy conformers.

Isoamyl alcohol (mostly gt)			
IR (cm^{-1})	Raman (cm^{-1})	calcd. (DFT) (cm^{-1})	obs./calcd.
3335 vs		3843	0.87
3326 sh,vs		still OH stretch	
	2966 s	3075	0.96
2959 s		3024	0.98
2931 s		3016	0.97
	2921 s	3016	0.97
	2875 s	3005	0.96
2874 m		2987	0.96
	2727 w	2982	0.91
1465 s	1469 m	1487	0.99
	1456 m	1470	0.99
1426 m		1425	1.00
1384 s		1402	0.99
1368 s		1372	1.00
	1340 w	1354	0.99
	1310 w	1316	1.00
1262 w		1231	1.03
1214 m		1201	1.01
1169 m		1173 (tt)	1.00
1125 s	1133 w	1131	0.98
1059 vs		1044	1.01
1012 s		1024	0.99
967 s	973 w	990	0.98
939 sh,w		966	0.97
921 vw		933	0.99
899 w		892	1.01
	867 w	891 (gg)	0.97
	855 w	848	1.01
836 m		845 (gg)	0.99
772 m	769 m	742	1.04
760 sh		794 (tt)	0.96
669 br,s		no match found	
	448 w	415 (gg)	1.08

trans-trans one, has only an abundance of 24 %, while the abundance of *gauche-gauche* is 32 % and that of *gauche-trans* is 43 %. The abundance of the high-energy conformer *trans-cis* is only 2 %. Here the first label indicates the position of the C–O bond relative to the neighboring H_2C–C bond, while the second label indicates the position of the O–H bond relative to the H_2C–C bond. Interestingly the MP2 minimum is actually *gauche-trans*, the same which comes out as the one with highest abundance in DFT and MP4 SDQ calculations. Consequently we base all our following discussions on the *gauche-trans* conformer

Table 2. Continued.

tert-Amyl alcohol (mostly *gg*)			
IR (cm^{-1})	Raman (cm^{-1})	calcd. (DFT) (cm^{-1})	obs./calcd.
3614 sh		3816	0.94
3371 vs		still OH stretch	
2971 s	2973 s	3035	0.98
2941 s	2944 vs	3032	0.97
2928 m	2920 s	3018	0.97
2883 m		2997	0.96
1466 s		1475	0.99
1446 m		1422	1.02
1379 m		1412	0.98
1374 m		1403	0.98
1365 s		1377	0.99
1330 vs		1361	0.98
1277 s		1293	0.99
1188 m		1209	0.98
1167 m		1150	1.01
1060 s	1063 w	1079	0.98
1053 s		1057	1.00
1019 s		1007	1.01
1003 s		1001	1.00
985 s		993 (tg)	0.99
940 w	943 w	931	1.01
881 w	884 w	879	1.00
786 s		788	1.00
727 m	730 vvs	723	1.01
636 m, broad		no match found	
479 sh		488 (tt)	0.98
474 sh		466 (tt)	1.02

which has by far the highest abundance. The comparison between observed and calculated wavenumbers for both alcohols is given in Table 2. Obviously there is a good agreement between observed and calculated wavenumbers. However, for three of the observed wavenumbers no matches in the calculated spectrum could be found. It seems that the samples used to record the spectra contained some traces of impurities. Furthermore, the conformational equilibrium mixture for isoamyl alcohol obviously contains the *trans-trans*, the *gauche-gauche* and the *gauche-trans* conformers, because some wavenumbers had to be assigned to the calculated ones of those conformers.

The conformational equilibrium of *tert*-amyl alcohol contains six conformers, however, only three of them in appreciable abundancies. Those are the *gauche-gauche* conformer with 52 % abundance, the *trans-gauche* conformer with 33 % abundance and the *trans-trans* one with 13 % abundance, all three having lines in the spectrum which is dominated by the one lowest in energy (*gauche-gauche*). Here the first label indicates again the position of the C–O bond relative to the neighboring C_2C–C bond, while the second label indicates the position of the O–H bond relative to one of the neighboring H_2C–H bonds.

Table S3 lists the geometrical parameters calculated by DFT and MP2 for the two alcohols. Obviously the DFT and MP2 values do not differ too much from each other. The C–O bond length is 1.433 Å in isoamyl alcohol while with 1.444 Å it is considerably longer in *tert*-amyl alcohol, indicating that the environment of the CO bond, crowded with methyl groups in the latter, obviously forces the OH group away from the methyl group, thereby making the CO bond weaker. This is indicated by the PED (Table 3) of the two alcohols which shows the CO stretch at 1044 cm^{-1} in isoamyl alcohol and considerably lower at 942 cm^{-1} in *tert*-amyl alcohol.

Discussion of Spectra

Table 3 lists the contributions of the group coordinates (symmetry coordinates in case of symmetry) to all the normal modes of the two alcohols. Note that not all of these modes show up in the spectra which are shown in Figs. 2 – 4. In Table 3 the wavenumbers observed in the spectra are highlighted as bold face. Some of the normal modes, a few in isoamyl alcohol, more of them in *tert*-amyl alcohol, are seen in GAUSSVIEW as having just a localized contribution in one methyl group, while in the in-phase and out-of-phase group coordinates they are present with equal magnitude in two methyl groups. However, the PED in such cases shows the same phenomenon, by having entries of the same percentage numbers of both of these group coordinates, which in the corresponding normal mode cancels one of the methyl group vibrations out. Thus the localization shows up equally well in the PED and in the GAUSSVIEW animation. If in a normal mode there are an in-phase and an out-of-phase linear combination of the methyl group vibrations superimposed, then this superposition determines in which one of the two methyl groups the corresponding localized methyl group motion takes place. This is not in all cases obvious in the GAUSSVIEW animations, if there is a large number of group coordinates mixed in the same normal mode. Then these other coordinates might mask the localized methyl group motion in the animation. This is a clear shortcoming of GAUSSVIEW. The normal

Table 3. Calculated wavenumbers (all of them, bold face italic ones seen in the experimental spectra, DFT), Potential Energy Distributions (PED), only entries larger or equal 5% are listed, together with (for comparison) the GAUSSVIEW results[a] for *gauche-trans* isoamyl alcohol and *gauche-gauche tert*-amyl alcohol.

Wavenumber (DFT, cm^{-1})	PED[b] (DFT)	GAUSSVIEW (DFT)
	gauche-trans isoamyl alcohol	
3843	100% OH str (S_{28})	yes
3111	76% CH_3 as str iph (S_2)	yes
	40% CH_3 as str oph (S_{11})	loc
3081	36% CH_3 as str oph (S_{11})	yes
	35% CH_3 as str iph (S_3)	masked
	24% CH_3 as str iph (S_2)	loc
3077	59% CH_3 as str iph (S_3)	yes
	19% CH_3 as str oph (S_{12})	masked
	19% CH_3 as str iph (S_2)	masked
3075	76% CH_3 as str oph (S_{12})	yes
	9% CH_3 as str oph (S_{11})	masked
	8% CH_3 as str iph (S_2)	masked
	6% CH_3 as str iph (S_3)	masked
3049	88% CH_2 as str (S_{39})	yes
	6% CH_2 s str (S_{26})	masked
3024	73% CH_3 s str iph(S_1)	yes
	13% CH_3 s str oph (S_{10})	masked
	7% CH_2 s str (S_{26})	masked
3016	39% CH_2 as str (S_{40})	yes
	38% CH_2 s str (S_{26})	yes
	10% CH_3 s str iph (S_1)	yes
	8% CH_2 as str (S_{39})	masked
3016	80% CH_3 s str oph (S_{10})	yes
	8% CH_2 s str (S_{26})	masked
	8% CH_3 s str iph(S_1)	masked
3005	53% CH_2 as str (S_{40})	yes
	27% CH_2 s str (S_{26})	masked
	6% *tert*-CH str (S_{47})	yes
	6% CH_3 s str iph (S_1)	yes
2987	85% *tert*-CH str (S_{47})	yes
	7% CH_2 s str (S_{26})	yes
2982	88% CH_2 s str (S_{27})	yes
	6% CH_2 s str (S_{26})	yes
1525	78% CH_2 scissor (S_{31})	yes
	11% CH_3 as def iph (S_7)	masked
	7% CH_3 as def oph (S_{16})	masked
1513	65% CH_3 as def iph (S_7)	indist
	15% CH_3 as def iph (S_5)	indist
	7% CH_3 rock (S_8)	hard
	6% CH_2 scissor (S_{31})	indist
1506	66% CH_3 as def iph (S_5)	indist
	12% CH_3 as def iph (S_7)	indist
	8% CH_2 scissor (S_{31})	indist
	7% CH_3 rock iph (S_6)	indist
1494	73% CH_3 as def oph (S_{16})	indist
	8% CH_2 scissor (S_{31})	indist
	7% CH_3 as def oph (S_{14})	indist
	5% CH_3 rock oph (S_{31})	indist
1487	83% CH_3 as def oph (S_{14})	indist
	9% CH_3 as def oph (S_{16})	indist
	6% CH_3 rock oph (S_{15})	indist
1470	92% CH_2 scissor (S_{30})	yes
1447	67% CH_2 wag (S_{33})	yes
	13% C-OH ipl bend(S_{34})	yes
1425	81% CH_3 s def iph (S_4)	yes
	10% CH_2 wag (S_{32})	hard
1402	90% CH_3 s def iph (S_{13})	yes
1392	46% CH_2 wag (S_{32})	yes
	19% CCC bend (S_{22})	yes
	15% CH_3 s def iph (S_4)	yes
	10% CH_2 wag (S_{33})	yes
1372	36% CC_2 rock (S_{25})	yes
	17% CH_2 twist (S_{41})	indist
	15% CC_2 twist (S_{24})	hard
	6% CH_3 s def iph (S_{13})	hard
1354	26% CCC bend (S_{22})	hard
	16% CC_2 wag (S_{23})	hard
	12% CH_2 twist (S_{42})	indist
	10% CH_2 wag (S_{32})	indist
	6% CC_2 rock (S_{25})	hard
	6% CC_2 as str (S_{35})	hard
1316	38% CH_2 twist (S_{41})	yes
	16% C-OH ipl bend (S_{34})	yes
	15% CH_2 twist (S_{42})	indist
	8% CC_2 twist (S_{24})	hard
	6% CC_2 rock (S_{25})	hard
1256	58% CH_2 twist (S_{42})	hard
	9% CH_2 twist (S_{41})	hard
	9% CH_2 rock (S_{45})	indist
	6% CH_2 wag (S_{32})	hard
1231	35% C-OH ipl bend (S_{34})	yes
	11% CH_2 wag (S_{33})	hard
	8% CH_2 twist (S_{41})	hard
	7% CH_3 rock iph (S_6)	hard
	6% CC_2 twist (S_{24})	hard
	6% CH_2 rock (S_{44})	hard
1201	24% CH_3 rock iph (S_8)	yes
	17% CH_3 rock iph (S_6)	indist
	12% CC_2 scissor (S_{21})	yes
	10% CC_2 s str (S_{19})	yes
	8% C–OH ipl bend (S_{34})	yes
	6% CCC as str (S_{35})	yes
1152	20% CH_2 rock (S_{45})	yes
	19% CH_3 rock iph (S_6)	indist
	11% CC_2 as str (S_{35})	yes
	11% CC_2 bend (S_{22})	indist
	10% CH_3 rock iph (S_8)	yes
	8% CCC ipl bend (S_{38})	yes
1131	18% CCC as str (S_{20})	yes
	15% CO str (S_{29})	yes
	11% CH_2 rock (S_{44})	yes
	10% CH_3 rock oph (S_{17})	yes
	8% C–OH ipl bend (S_{34})	hard
	7% CH_2 twist (S_{41})	hard
	5% CC_2 twist (S_{24})	indist
1044	41% CO str (S_{29})	yes

Table 3. Continued.

Wavenumber (DFT, cm^{-1})	PED[b] (DFT)	GAUSSVIEW (DFT)
	18 % CCC as str (S_{35})	yes
	12 % CH_3 rock iph (S_8)	yes
	7 % CCC s str (S_{36})	indist
	6 % CH_3 rock iph (S_6)	indist
1024	35 % CH_2 rock (S_{45})	indist
	9 % CH_2 wag (S_{32})	indist
	8 % CH_3 rock iph (S_6)	indist
	8 % CCC as str (S_{35})	indist
	5 % CCC s str (S_{36})	indist
	5 % CH_3 rock iph (S_8)	indist
	5 % CCC as str (S_{20})	indist
990	19 % CCC as str (S_{20})	yes
	19 % CCC as str (S_{35})	yes
	17 % CO str (S_{29})	yes
	11 % CH_3 rock iph (S_8)	yes
	11 % CH_2 rock (S_{44})	yes
	6 % CH_2 twist (S_{41})	hard
966	45 % CH_3 rock oph (S_{17})	indist
	26 % CC_2 as str (S_{20})	yes
	17 % CH_3 rock oph (S_{15})	indist
933	57 % CH_3 rock oph (S_{15})	indist
	20 % CH_3 rock oph (S_{17})	yes
	9 % CC_2 rock (S_{25})	hard
892	41 % CC_2 s str (S_{19})	yes
	21 % CC_2 s str (S_{36})	yes
	11 % CH_2 rock (S_{45})	yes
	10 % CH_3 rock iph (S_8)	yes
848	43 % CH_2 rock (S_{44})	yes
	18 % CO str (S_{29})	yes
	7 % CC_2 as str (S_{35})	indist
742	50 % CC_2 s str (S_{36})	yes
	33 % CCC s str (S_{19})	yes
566	29 % CC_2 wag (S_{23})	yes
	25 % CCC ipl bend (S_{38})	yes
	13 % CCO ipl bend (S_{37})	yes
	8 % CH_3 rock iph (S_6)	yes
	7 % CH_2 rock (S_{45})	indist
	6 % CH_2 rock (S_{44})	indist
410	39 % CCO ipl bend (S_{37})	yes
	13 % CCC scissor (S_{21})	yes
	11 % CH_2 rock (S_{44})	yes
	8 % CCC wag (S_{23})	indist
	7 % CCC rock (S_{25})	indist
	7 % CCC twist (S_{24})	indist
371	57 % CC_2 scissor (S_{21})	indist
	11 % CC_2 twist (S_{24})	indist
	10 % CC_2 rock (S_{25})	indist
343	19 % CC_2 twist (S_{24})	indist
	17 % CCC rock (S_{23})	indist
	16 % CCO ipl bend (S_{37})	indist
	14 % CCC rock (S_{25})	indist
	14 % CC_2 scissor (S_{21})	indist
289	72 % OH torsion (S_{43})	yes
265	29 % CH_3 torsion oph (S_{18})	yes
	21 % CH_3 torsion iph (S_9)	indist
	19 % OH torsion (S_{43})	yes

Table 3. Continued.

Wavenumber (DFT, cm^{-1})	PED[b] (DFT)	GAUSSVIEW (DFT)
	12 % CCC ipl bend (S_{38})	hard
	6 % CO torsion (S_{46})	hard
251	63 % CH_3 torsion oph (S_{18})	yes
	6 % CH_3 torsion iph (S_9)	indist
	6 % CH_3 as def oph (S_{24})	indist
	5 % CCC ipl bend (S_{38})	indist
231	55 % CH_3 torsion iph (S_9)	yes
	26 % CC_2 ipl bend (S_{38})	hard
	7 % CCC wag (S_{23})	hard
	5 % CCO ipl bend (S_{37})	yes
152	53 % CO torsion (S_{46})	yes
	24 % isopropyl torsion (S_{46})	hard
	12 % CH_3 torsion iph (S_9)	yes
	5 % CCC ipl bend (S_{38})	yes
43	71 % isopropyl torsion (S_{48})	yes
	28 % CO torsion (S_{46})	yes
	gauche-gauche tert-amyl alocohol	
3816	100 % OH str (S_{45})	yes
3118	36 % CH_3 as str oph (S_{12})	yes
	34 % CH_3 as str iph (S_3)	loc
	14 % CH_3 as str iph (S_2)	loc
	12 % CH_3 as str oph (S_1)	loc
3106	66 % CH_3 as str iph (S_2)	yes
	19 % CH_3 as str oph (S_{12})	loc
	9 % eth CH_3 as str (S_{38})	yes
3103	76 % eth CH_3 as str (S_{38})	yes
	11 % CH_3 as str iph (S_2)	yes
	10 % eth CH_3 as str (S_{30})	masked
3098	82 % CH_3 as str oph (S_{11})	yes
	12 % CH_3 as str iph (S_3)	loc
	5 % CH_3 as str iph (S_2)	loc
3089	86 % eth CH_3 as str (S_{30})	yes
	11 % eth CH_3 as str (S_{38})	indist
3079	48 % CH_3 as str iph (S_3)	yes
	41 % CH_3 as str oph (S_{12})	loc
3040	51 % CH_3 s str iph (S_1)	yes
	31 % CH_3 s str oph (S_{10})	loc
	8 % CH_2 as str (S_{37})	yes
3035	71 % CH_2 as str (S_{37})	yes
	10 % CH_2 s str (S_{26})	yes
	9 % CH_3 s str iph (S_1)	yes
	6 % CH_3 s str oph (S_{10})	loc
3032	92 % eth CH_3 s str (S_{29})	yes
3018	60 % CH_3 s str oph (S_{10})	yes
	33 % CH_3 s str iph (S_1)	loc
2997	83 % CH_2 s str (S_{26})	yes
	13 % CH_2 as str (S_{37})	indist
1517	33 % eth CH_3 as def (S_{41})	yes
	29 % CH_3 as def oph (S_{16})	yes
	20 % CH_3 as def iph (S_5)	indist
	5 % CH_3 as def iph (S_7)	indist
1510	33 % eth CH_3 as def (S_{41})	yes
	20 % eth CH_3 as def (S_{34})	indist
	15 % CH_3 as def iph (S_5)	yes
	14 % CH_2 scissor (S_{27})	yes
	8 % CH_3 as def oph (S_{16})	indist

Table 3. Continued.

Wavenumber (DFT, cm^{-1})	PED[b] (DFT)	GAUSSVIEW (DFT)
1501	46 % CH_3 as def oph (S_{16})	yes
	18 % CH_3 as def iph (S_5)	indist
	8 % eth CH_3 as def (S_{34})	yes
	6 % eth CH_3 as def (S_{41})	indist
	5 % CH_3 as def iph (S_7)	indist
1499	58 % eth CH_3 as def (S_{34})	yes
	13 % CH_3 as def iph (S_5)	yes
	9 % CH_3 as def oph (S_{14})	loc
	7 % CH_2 scissor (S_{27})	yes
1492	37 % CH_3 as def iph (S_7)	yes
	28 % CH_2 scissor (S_{27})	yes
	21 % CH_3 as def iph (S_5)	indist
1485	35 % CH_3 as def oph (S_{14})	yes
	30 % CH_3 as def iph (S_5)	indist
	15 % CH_2 scissor (S_{27})	yes
	8 % eth CH_3 as def (S_{41})	yes
1475	45 % CH_3 as def oph (S_{14})	yes
	34 % CH_2 scissor (S_{27})	yes
	10 % CH_3 as def iph (S_7)	loc
1422	72 % CH_3 s def iph (S_4)	yes
	5 % CH_2 wag (S_{28})	yes
1412	90 % eth CH_3 s def (S_{33})	yes
1403	69 % CH_3 s def oph (S_{13})	yes
	13 % CH_3 s def iph (S_4)	loc
	6 % CC_2 as str (S_{20})	yes
1377	38 % CH_2 wag (S_{28})	yes
	18 % CH_3 s def oph (S_{13})	yes
	10 % C–OH ipl bend (S_{46})	yes
	9 % CH_3 as def oph (S_{14})	indist
	6 % CH_2 twist (S_{39})	indist
1361	31 % CH_2 wag (S_{28})	yes
	18 % C–OH ipl bend (S_{46})	yes
	11 % CH_2 twist (S_{39})	indist
	7 % eth CCC as str (S_{32})	yes
	5 % CH_3 s def oph (S_{13})	yes
1293	51 % CH_2 twist (S_{39})	yes
	14 % eth CH_3 rock (S_{42})	yes
	13 % C–OH ipl bend (S_{46})	yes
1231	38 % CH_3 rock iph (S_6)	yes
	13 % CC_2 wag (S_{23})	yes
	8 % eth CCC as str (S_{32})	yes
	7 % CH_3 as def iph (S_5)	loc
	6 % CH_2 wag (S_{28})	yes
	6 % eth CCC s str (S_{31})	indist
1209	29 % CH_3 rock oph (S_{17})	yes
	11 % CH_2 rock (S_{40})	yes
	10 % eth CCC rock (S_{42})	yes
	8 % CO str (S_{44})	yes
	7 % CC_2 scissor (S_{21})	yes
	7 % CC_2 s str (S_{19})	yes
1150	34 % C–OH ipl bend (S_{46})	yes
	14 % eth CH_3 rock (S_{35})	yes
	11 % CC_2 as str (S_{20})	yes
	8 % CH_3 rock oph (S_{15})	yes
	7 % eth CCC ipl bend (S_{36})	yes
	6 % CC_2 rock (S_{25})	hard

Table 3. Continued.

Wavenumber (DFT, cm^{-1})	PED[b] (DFT)	GAUSSVIEW (DFT)
	6 % CH_2 rock (S_{40})	hard
1079	24 % CH_3 rock oph (S_{17})	yes
	17 % eth CH_3 rock (S_{42})	yes
	15 % eth CCC as str (S_{32})	yes
	12 % CH_2 rock (S_{40})	hard
	12 % CH_2 twist (S_{39})	indist
1057	19 % eth CH_3 rock (S_{35})	yes
	18 % CH_3 rock iph (S_8)	yes
	18 % CC_2 as str (S_{20})	yes
	11 % eth CCC as str (S_{32})	yes
	8 % C–OH ipl bend (S_{46})	yes
	7 % eth CCC s str (S_{31})	indist
1007	42 % eth CCC as str (S_{32})	yes
	18 % CH_3 rock iph (S_6)	yes
	10 % CH_2 wag (S_{28})	yes
	8 % CH_3 rock iph (S_6)	yes
1001	72 % CH_3 rock oph (S_{15})	yes
	11 % eth CH_3 rock (S_{35})	yes
942	34 % CO str (S_{44})	yes
	27 % eth CCC s str (S_{31})	yes
	18 % CH_3 rock oph (S_{17})	yes
	6 % eth CH_3 rock (S_{42})	yes
931	52 % CH_3 rock iph (S_8)	yes
	6 % CC_2 wag (S_{23})	indist
	5 % CH_3 rock oph (S_{15})	indist
879	31 % CO str (S_{44})	yes
	25 % eth CCC s str (S_{31})	yes
	24 % CH_3 rock iph (S_6)	yes
	11 % CC_2 s str (S_{19})	yes
788	55 % CH_2 rock (S_{40})	yes
	31 % eth CH_3 rock (S_{42})	yes
723	37 % CC_2 s str (S_{19})	yes
	27 % eth CCC s str (S_{31})	yes
	14 % CO str (S_{44})	yes
	9 % eth CCC as str (S_{32})	masked
	6 % eth CH_3 rock (S_{35})	hard
528	23 % CCC ipl bend (S_{22})	yes
	20 % CC_2 rock (S_{25})	indist
	18 % eth CCC ipl bend (S_{36})	yes
	8 % CC_2 as str (S_{20})	yes
	6 % CC_2 s str (S_{19})	indist
	6 % CC_2 wag (S_{23})	indist
454	42 % CC_2 rock (S_{25})	yes
	17 % CCC ipl bend (S_{22})	yes
	7 % CC_2 scissor (S_{21})	indist
	7 % CC_2 wag (S_{23})	indist
	6 % CC_2 as str (S_{20})	indist
415	67 % CC_2 wag (S_{23})	yes
	10 % CC_2 scissor (S_{21})	indist
	6 % CH_3 rock oph (S_{17})	yes
367	41 % CC_2 twist (S_{24})	yes
	21 % CC_2 scissor (S_{21})	indist
	17 % eth CCC ipl bend (S_{36})	yes
	7 % eth CCC s str (S_{31})	no
345	38 % CC_2 scissor (S_{21})	yes
	9 % CC_2 twist (S_{24})	hard

Table 3. Continued.

Wavenumber (DFT, cm^{-1})	PED[b] (DFT)	GAUSSVIEW (DFT)
	17 % CC_2 twist (S_{24})	indist
298	79 % tert OH torsion (S_{47})	yes
	18 % CH_3 torsion oph (S_{18})	yes
270	34 % CH_3 torsion oph (S_{18})	yes
	22 % eth CH_3 torsion (S_{43})	yes
	10 % CC_2 twist (S_{24})	indist
	9 % eth CCC ipl bend (S_{36})	hard
	8 % tert OH torsion (S_{47})	yes
	6 % CC_2 rock (S_{25})	indist
255	35 % CH_3 torsion oph (S_{18})	yes
	32 % CH_3 torsion iph (S_9)	loc
	11 % eth CCC ipl bend (S_{36})	yes
	9 % CC_2 twist (S_{24})	hard
	5 % tert OH torsion (S_{47})	yes
227	42 % CH_3 torsion iph (S_9)	yes
	22 % eth CCC ipl bend (S_{36})	yes
	10 % CC_2 twist (S_{24})	indist
	8 % CCC ipl bend (S_{22})	indist
	6 % CC_2 rock (S_{25})	indist
207	60 % eth CH_3 torsion (S_{43})	yes
	20 % CH_3 torsion iph (S_9)	yes
	8 % CH_3 torsion oph (S_{18})	hard
111	91 % hydr. isopr. tors. (S_{48})	yes
	6 % eth CH_3 torsion (S_{43})	yes

[a] "hard" means hard to see, almost invisible, "masked" means invisible because of a similar coordinate with much larger amplitude motion, "yes" means clearly visible, "no" means invisible, "indist" means indistinguishable from others, "loc" localization of motion in one side of the molecule; [b] abbreviations: str: stretch, def: deformation, s: symmetric, as: antisymmetric, iph: in phase, oph: out of phase, ipl: in plane, opl: out of plane.

mode with the highest calculated wavenumber is the one at 3843 cm^{-1} in isoamyl alcohol and at 3816 cm^{-1} in *tert*-amyl alcohol, both being OH stretches with 100 % PED in both alcohols, S_{28} in isoamyl alcohol and S_{45} in *tert*-amyl alcohol. As usual these OH stretches show up at lower wavenumbers in the infrared spectra, namely at 3335 cm^{-1} in isoamyl alcohol and at 3614 cm^{-1} in *tert*-amyl alcohol. In both spectra at 3326 and at 3371 cm^{-1} there are shoulders which have no counterparts among the calculated normal modes. Most probably these are due to OH stretches, either hydrogen bonded ones or from crystal water. The next lower calculated wavenumber in isoamyl alcohol is at 3075 cm^{-1} and has a highly mixed PED with a leading contribution of 76 % out-of-phase methyl antisymmetric stretch (S_{12}). In the GAUSSVIEW animation three of the four PED entries are masked by the leading one and cannot be identified. There is no counterpart to this mode in the experimental spectra of *tert*-amyl alcohol. For isoamyl alcohol the line is observed in the Raman spectrum at 2966 cm^{-1} as a strong one. The CH stretches in isoamyl alcohol continue at 3024 cm^{-1} with a leading term of 73 % symmetric in-phase CH_3 stretch (S_1), at 3016 cm^{-1} with two lines, one being highly mixed with leading terms of 39 % CH_2 antisymmetric stretch (S_{40}) and of 38 % CH_2 symmetric stretch (S_{26}), the other one being more pure with a leading 80 % out-of-phase methyl symmetric stretch (S_{10}), at 3005 cm^{-1} with 53 % CH_2 antisymmetric stretch (S_{40}), at 2987 cm^{-1} with 85 % *tert*-CH stretch (S_{47}), and finally at 2982 cm^{-1} with 88 % CH_2 symmetric stretch (S_{27}). These lines are observed between 2966 and 2727 cm^{-1}, all strong, some even very strong bands, besides the last one which is a medium one. In the GAUSSVIEW animation most of the smaller PED entries cannot be seen. In *tert*-amyl alcohol the line at 3035 cm^{-1} has a PED of 71 % CH_2 antisymmetric stretch (S_{37}). Below that at 3032 cm^{-1} there is a mode with 92 % ethyl CH_3 symmetric stretch (S_{29}), at 3018 cm^{-1} there is a mixed mode with 60 % out-of-phase methyl symmetric stretch (S_{10}) and 33 % in-phase methyl symmetric stretch (S_1), which cannot be seen in the GAUSSVIEW animation, and finally at 2997 cm^{-1} 83 % CH_2 symmetric stretch (S_{26}). These lines are observed between 2971 and 2883 cm^{-1} in the infrared and Raman spectra with most being strong or even very strong features.

In the lower wavenumber region we want to focus on the intense and characteristic lines. The next strong line in the infrared spectrum of isoamyl alcohol is one at 1465 cm^{-1} which is calculated at 1487 cm^{-1} with 83 % PED for an out-of-phase methyl antisymmetric deformation (S_{14}). In the infrared spectrum of *tert*-amyl alcohol there is a similar strong band observed also at 1466 cm^{-1} and calculated at 1475 cm^{-1}. Because *tert*-amyl alcohol is *gauche-gauche*, there are fewer symmetry restrictions for the mixing of group coordinates in a normal mode, and thus in the PED of this mode the leading contribution (same as above, S_{14}) has only 45 %, while there is a PED entry of 34 % for the methylene scissor (S_{27}) motion. Note that the Raman spectra contain, besides the CH stretches, only medium and weak intensity lines, except for a very strong one in *tert*-amyl alcohol (see below).

In the infrared spectrum of isoamyl alcohol one sees a group of five strong to weak bands at 1262, 1214, 1169, 1125, and 1059 cm^{-1}, which are calculated

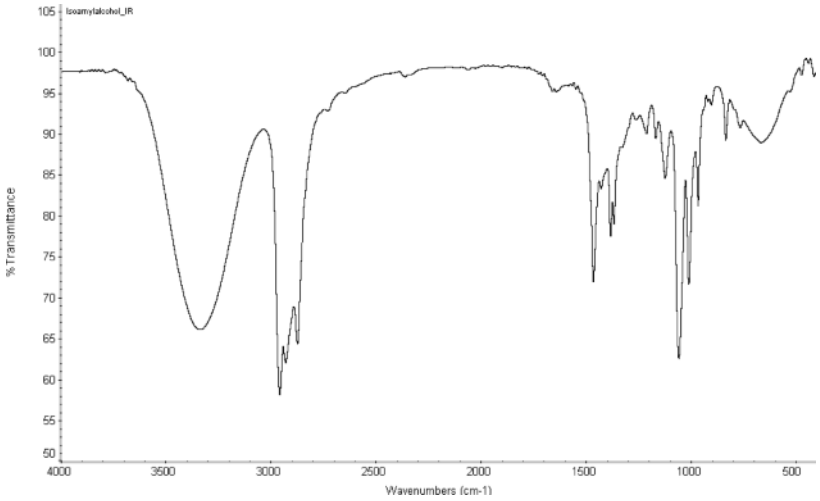

Fig. 2. Infrared spectrum of liquid isoamyl alcohol as obtained in our laboratory.

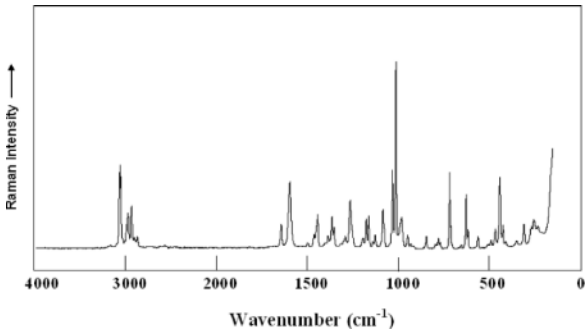

Fig. 3. Raman spectrum of isoamyl alcohol retrieved from http://www.aist.go.jp/RIODB/SDBS; no. 541 (accessed March 20, 2013).

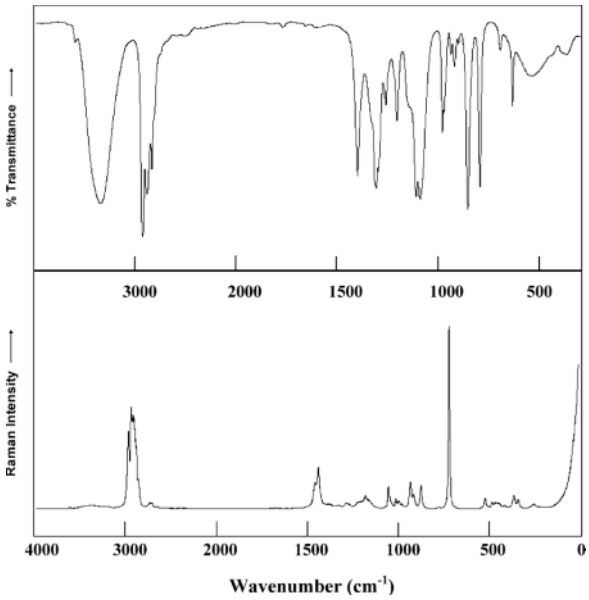

Fig. 4. Infrared (upper) and Raman (lower) spectra of liquid *tert*-amyl alcohol retrieved from http://www.aist.go.jp/RIODB/SDBS; no. 1709 (accessed March 20, 2013).

between 1231 and 1044 cm^{-1}, where the 1214 cm^{-1} band has to be assigned to the calculated mode at 1201 cm^{-1} in the *trans-trans* conformer. Of these bands the one with highest wavenumber has a PED of 58 % methylene twist (S_{42}), while the band calculated at 1231 cm^{-1} is highly mixed with 35 % C–OH in plane bend (S_{34}) and 11 % methylene wag (S_{33}). The band calculated at 1201 cm^{-1} is again highly mixed with leading terms of 24 % in-phase methyl rock (S_8) and 17 % of also in-phase methyl rock (S_6, another coordinate describing also in phase methyl rock). These two cannot be seen separately in the GAUSSVIEW animation. The next lower calculated bands at 1131, 1044 and 1024 cm^{-1} are all highly mixed again as can be seen from the rather low leading contributions, which are 18 % CCC antisymmetric stretch (S_{20}) in the 1131 cm^{-1} band, followed by 15 % CO stretch (S_{29}), 41 % CO stretch (S_{29}) in the 1044 cm^{-1} band, and 35 % methylene rock (S_{45}) in the 1024 cm^{-1} band. For *tert*-amyl alcohol this series of neighboring strong and very strong bands in the infrared spectrum is interrupted by two bands of medium intensity observed at 1188 and 1167 cm^{-1}. The strong and very strong bands in the infrared spectrum of *tert*-amyl alcohol are observed at 1365, 1330, 1277, 1060, 1053, 1019,

1003, and 985 cm^{-1} and calculated between 1377 and 1001 cm^{-1}, while the 985 cm^{-1} band has to be assigned to the calculated 993 cm^{-1} band in the *gauche-trans* conformer. The degree of mixing of group coordinates in these normal modes in *tert*-amyl alcohol is even larger than in isoamyl alcohol, so that we list only the leading PED entries in the corresponding calculated normal modes. These are 38 % methylene wag (S_{28}) in the 1377 cm^{-1} band and 31 % of the same coordinate (S_{28}) in the 1361 cm^{-1} band. The calculated 1293 cm^{-1} band is more pure and has 51 % methylene twist (S_{39}) as leading PED entry. The leading PED entry in the band calculated at 1079 cm^{-1} is of only 24 % out-of-phase methyl rock (S_{17}), as much as in the case of the corresponding bands in isoamyl alcohol. For *tert*-amyl alcohol, in the band at 1057 cm^{-1} the leading PED term is even smaller, namely 19 % ethylmethyl rock (S_{35}), while the one in the 1007 cm^{-1} band is 42 % ethyl CCC symmetric stretch (S_{32}). The 1001 cm^{-1} band is much more pure with a leading PED term of 72 % out-of-phase methyl rock (S_{15}).

Below this group of strong features, there is only one more strong band observed in the infrared spectrum of isoamyl alcohol at 772 cm^{-1}, calculated at 742 cm^{-1}. This is a relatively pure normal mode with 50 % and 33 % CCC symmetric stretch (different coordinates: S_{19} and S_{36}). For *tert*-amyl alcohol only one more remarkable feature is observed, namely the very strong Raman line at 730 cm^{-1}, calculated at 723 cm^{-1}. With 27 % CCC symmetric stretch (S_{19}) and 27 % ethyl CCC symmetric stretch (S_{31}) this line has a similar PED as the lowest strong infrared band in isoamyl alcohol observed at 772 cm^{-1}. Note that "CCC symmetric stretch" denotes the symmetric combination of the two C–C stretches in the CH_3–CH–CH_3 subgroup in isoamyl alcohol and the corresponding stretches in the CH_3–COH–CH_3 subgroup in *tert*-amyl alcohol, while "ethyl CCC symmetric stretch" denotes the symmetric combination of the two C–C stretches in the $C_2C_3C_6$ subgroup in isoamyl alcohol and in the $C_2C_1C_{15}$ subgroup in *tert*-amyl alcohol.

Conclusion

The spectra of isoamyl alcohol and *tert*-amyl alcohol are rather similar with straightforward assignments of lines. The calculated lines in both cases fit nicely to the experimental ones. The calculated spectra of amylalcohol, as a primary alcohol like isoamyl alcohol, contain not much new data, and thus we refrain from discussing them here in any detail. Both the CO and the OH bond appear to be weaker in the tertiary than in the primary alcohol. This is indicated by the CO stretch wavenumbers which are lower in the tertiary alcohol (879 and 942 cm^{-1}) than in the primary alcohol (990 and 1044 cm^{-1}). The OH stretch in the latter case is also higher (3843 cm^{-1}) than in the former (3816 cm^{-1}). The corresponding bonds are longer in the tertiary than in the primary alcohol (although the difference in bond length of the OH bond in *tert*-amyl alcohol is very small). We attribute that to steric effects in the tertiary alcohol.

Supporting information

Internal coordinate definitions, group coordinates, and calculated (DFT and MP2) structural parameters, dipole moments and rotational constants are given as Supporting Information available online (DOI: 10.5560/ZNB.2013-3003).

Acknowledgement

The support by the Chemistry Department of King Fahd University of Petroleum and Minerals (KFUPM) is highly acknowledged.

[1] Our PED program, written by one of us (WF), based on W. Förner, *Intern. J. Quantum Chem.* **2004**, *99*, 533 – 555.
[2] R. Dennington II, T. Keith, J. Millam, K. Eppinnett, W. L. Hovell, R. Gilliland, GAUSSVIEW (version 3.0), Semichem, Inc., Shawnee Mission, KS (USA) **2003**.
[3] N. Yamashita, T. Motoyoshi, A. Nishimura, *J. Biosci. Bioeng.* **2000**, *89*, 522 – 527.
[4] L. F. Ribeiro Pinto, *Toxicology* **2000**, *151*, 73 – 79.
[5] T. Fukushige, T. Yonezawa, Y. Sakai, K. Okawa, A. Iwamatsu, H. Sone, Y. Tamai, *J. Biosci. Bioeng.* **2001**, *92*, 83 – 85.
[6] K. Kern, C. D. Nunn, A. Pichove, J. R. Dickinson, *FEMS Yeast Res.* **2004**, *5*, 43 – 49.
[7] K. Hirooka, Y. Yamamoto, N. Tsutsui, T. Tanaka, *J. Biosci. Bioeng.* **2005**, *99*, 125 – 129.

[8] D. McGinty, A. Lapczynski, J. Scognamiglio, C. S. Letizia, A. M. Api, *Food Chem. Toxicol.* **2010**, *48*, S102–S109.
[9] C.-Y. Shiau, S. Chen, J. C. Tsai, S. I. Lin, *Appl. Catalysis* **2000**, *A198*, 95 – 102.
[10] H. T. R. Teo, B. Saha, *J. Catalysis* **2004**, *228*, 174 – 182.
[11] W.-Q. Zhuang, J.-H. Tay, S. Yi, S. T.-L. Tay, *J. Biotech.* **2005**, *118*, 45 – 53.
[12] R. Gonzalez-Olmos, M. Iglesias, *Chemosphere* **2008**, *71*, 2098 – 2105.
[13] W. Kiatkittipong, P. Intaracharoen, N. Laosiripojana, C. Chaisuk, P. Praser-trhdam, S. Assabumrungrat, *Comput. Chem. Eng.* **2011**, *35*, 2034 – 2043.
[14] C. Alonso, C. R. Chamorro, J. J. Segovia, M. C. Martin, E. A. Montero, M. A. Villamanam, *Fluid Phase Equilib.* **2004**, *217*, 145 – 155.
[15] F. Aiouache, S. Goto, *Chem. Eng. Sci.* **2003**, *58*, 2465 – 2477.
[16] G. D. Yadav, G. S. Pathre, *Appl. Catal.* **2006**, *297A*, 237 – 246.
[17] D. W. Kim, H.-J. Yeong, S. T. Lim, M.-H. Sohn, D. Y. Chi, *Tetrahedron* **2008**, *64*, 4209 – 4214.
[18] D. W. Kim, H.-J. Jeong, S. T. Lim, M.-H. Sohn, *Tetrahedron Lett.* **2010**, *51*, 432 – 434.
[19] O. Boonthamtirawuti, W. Kiatkittipong, A. Arpornwichanop, P. Prasertham, S. Assabumrungrat, *J. Ind. Eng. Chem.* **2009**, *15*, 451 – 457.
[20] M. J. Frisch, G. W. Trucks, H. B. Schlegel, G. E. Scuseria, M. A. Robb, J. R. Cheeseman, J. A. Montgomery, Jr., T. Vreven, K. N. Kudin, J. C. Burant, J. M. Millam, S. S. Iyengar, J. Tomasi, V. Barone, B. Mennucci, M. Cossi, G. Scalmani, N. Rega, G. A. Petersson, H. Nakatsuji, M. Hada, M. Ehara, K. Toyota, R. Fukuda, J. Hasegawa, M. Ishida, T. Nakajima, Y. Honda, O. Kitao, H. Nakai, M. Klene, X. Li, J. E. Knox, H. P. Hratchian, J. B. Cross, V. Bakken, C. Adamo, J. Jaramillo, R. Gomperts, R. E. Stratmann, O. Yazyev, A. J. Austin, R. Cammi, C. Pomelli, J. W. Ochterski, P. Y. Ayala, K. Morokuma, G. A. Voth, P. Salvador, J. J. Dannenberg, V. G. Zakrzewski, S. Dapprich, A. D. Daniels, M. C. Strain, O. Farkas, D. K. Malick, A. D. Rabuck, K. Raghavachari, J. B. Foresman, J. V. Ortiz, Q. Cui, A. G. Baboul, S. Clifford, J. Cioslowski, B. B. Stefanov, G. Liu, A. Liashenko, P. Piskorz, I. Komaromi, R. L. Martin, D. J. Fox, T. Keith, M. A. Al-Laham, C. Y. Peng, A. Nanayakkara, M. Challacombe, P. M. W. Gill, B. Johnson, W. Chen, M. W. Wong, C. Gonzalez, J. A. Pople, GAUSSIAN 03 (revision E.01), Gaussian, Inc., Wallingford CT (USA) **2004**.